Comparison of SIVmac239$_{(352-382)}$ and SIVsmmPBj41$_{(360-390)}$ enterotoxic synthetic peptides

C.L. Swaggerty,[a,1] H. Huang,[b] W.S. Lim,[a] F. Schroeder,[b] and J.M. Ball[a,*]

[a] Department of Pathobiology, College of Veterinary Medicine, Texas A&M University, TAMU 4467, College Station, TX 77843-4467, USA
[b] Department of Physiology and Pharmacology, College of Veterinary Medicine, Texas A&M University, College Station, TX 77843-4466, USA

Abstract

To characterize the active domain of the simian immunodeficiency virus (SIV) surface unit (SU) enterotoxin, peptides corresponding to the V3 loop of SIVmac239 (SIVmac) and SIVsmmPBj41 (SIVpbj) were synthesized and examined for enterotoxic activity, α-helical structure, and interaction(s) with model membranes. SIVmac and SIVpbj induced a dose-dependent diarrhea in 6–8-day-old mouse pups similar to full-length SU. The peptides mobilized $[Ca^{2+}]_i$ in HT-29 cells with distinct oscillations and elevated inositol triphosphate levels. Circular dichroism analyses showed the peptides were predominantly random coil in buffer, but increased in α-helical content when placed in a hydrophobic environment or with cholesterol-containing membrane vesicles that are rich in anionic phospholipids. None of the peptides underwent significant secondary structural changes in the presence of neutral vesicles indicating ionic interactions were important. These data show that the SIV SU enterotoxic domain localizes in part to the V3 loop region and interacts with anionic membrane domains on the host cell surface.
© 2004 Elsevier Inc. All rights reserved.

Keywords: SIVmac239$_{(352-382)}$; SIVsmmPBj41$_{(360-390)}$; Enterotoxic synthetic peptides

Introduction

Alterations in gastrointestinal (GI) function, including chronic diarrhea, malabsorption, and significant weight loss, are devastating characteristics of human immunode-ficiency virus (HIV) or simian immunodeficiency virus (SIV) infection and account for the frequently observed wasting syndrome of acquired immunodeficiency syndrome (AIDS) or simian AIDS (SAIDS) (Ehrenpreis et al., 1992). There are numerous HIV or SIV cases in which secondary enteric pathogens cannot be identified as the causative agent of the diarrhea and wasting (Heise et al., 1991, 1993; Lambl et al., 1996; Ullrich et al., 1989); hence, it is plausible that the virus, viral replica-tion, or a viral protein is responsible for the (GI) dysfunction. In an earlier report, we showed purified SIVmac surface unit (SU) induces a dose-dependent diarrheal response in 6–8-day-old Balb/C mouse pups, promotes fluid accumulation in adult mouse intestinal loops in the absence of histological alterations, promotes chloride (Cl⁻) secretory currents across unstripped mouse intestinal mucosa as measured in Ussing chambers, and increases inositol triphosphate (IP3) and intracellular cal-cium ($[Ca^{2+}]_i$) levels in HT-29 colonic cells. These data fulfill the criteria of an enterotoxin making SIV SU the second viral enterotoxin to be described (Swaggerty et al., 2000).

Many diverse functions have been attributed to the envelope glycoproteins of HIV or SIV (Hunter and Swanstrom, 1990; Medina et al., 1999). SU determines the host range and cell tropism of the virus by functioning as the viral receptor. The envelope glycoproteins, SU and transmembrane (TM), also contribute to the cytopathicity of the virus by inducing cell lysis or syncytium formation of target cells (Hunter and Swanstrom, 1990). SU is weakly bound to TM and can freely dissociate leading to immune-mediated killing of uninfected target cells (Hunter and Swanstrom, 1990) or may contribute to GI dysfunction (Swaggerty et al., 2000).

The pathogenesis of SIV or HIV infections is very complex and not fully understood. The auxiliary *nef* gene overlaps *env* and contributes to disease in rhesus macaques (*Macaca mulatta*) (Alexander et al., 1999; Du et al., 1995; Kirchhoff et al., 1999; Lou and Peterlin, 1997; Sawai et al., 1996). SIVmac239 is a virus derived from an infectious molecular clone and causes a typical lentivirus infection with slow progression to disease that often results in SAIDS in infected macaques (Alexander et al., 1999; Kaur et al., 1998; Kestler et al., 1990; Naidu et al., 1988). However, SIVmac239 can undergo mutations that result in a highly pathogenic virus that causes severe GI dysfunction and disease. In many cases, the mutations occur in codon 17 of *nef* that causes a predicted amino acid change at residue 17 from Arg to Tyr, a pattern typically found in the acutely pathogenic SIVsmmPBj14 strain (Du et al., 1995; Kirchhoff et al., 1999; Lou and Peterlin, 1997).

SIVsmmPBj14 (SIVpbj14) is an atypical, pathogenic clone of SIV that causes an acute clinical syndrome characterized by depression, anorexia, fever, profuse diarrhea, dehydration, wasting, and death within 6–10 days post infection (Fultz et al., 1989; Lewis et al., 1992; Swanstrom and Wills, 1997). SIVpbj14 infects and causes disease in different strains of monkeys including the pig-tailed cynomolgus (*Macaca fascicularis*), sooty mangabeys (*Cercocebus atys*), and to a more variable degree, rhesus macaques (Fultz, 1994; Fultz et al., 1989; Lewis et al., 1992). The other SIV strains are generally species-specific in that symptoms rarely occur in multiple species. The extensive lymphoid hyperplasia of T cells, particularly in the gut-associated lymphoid tissues (GALT), is one of the most important pathological features associated with SIVpbj14 infections. Viral threshold in the GALT directs the disease course in infected pig-tailed macaques wherein a single log dilution difference determines if an animal succumbs to disease and dies (Fultz, 1994; Fultz et al., 1989). Because SIVpbj14 induces a high titer viremia, an extensive number of immune cells are activated, proliferate, and produce cytokines. The increased production of cytokines, in particular TNFα and IL-6, results in an acute inflammatory disease in the GI tract, hemorrhaging or bloody diarrhea, and intestinal tissue destruction (Farthing, 2000; Fultz and Zack, 1994; Fultz et al., 1989; Lewis et al., 1992). In addition to the GI dysfunction, infected pig-tailed macaques often deteriorate rapidly after the onset of anorexia or depression yet before the onset of diarrhea. The exact roles of inflammation and disease progression remain unclear. Virus has been isolated from lymphoid tissue such as the tonsils of SIVpbj14-infected monkeys in the complete absence of mucosal inflammation (Swanstrom and Wills, 1997). A high titer viremia during disease progression in SIVpbj14-infected monkeys
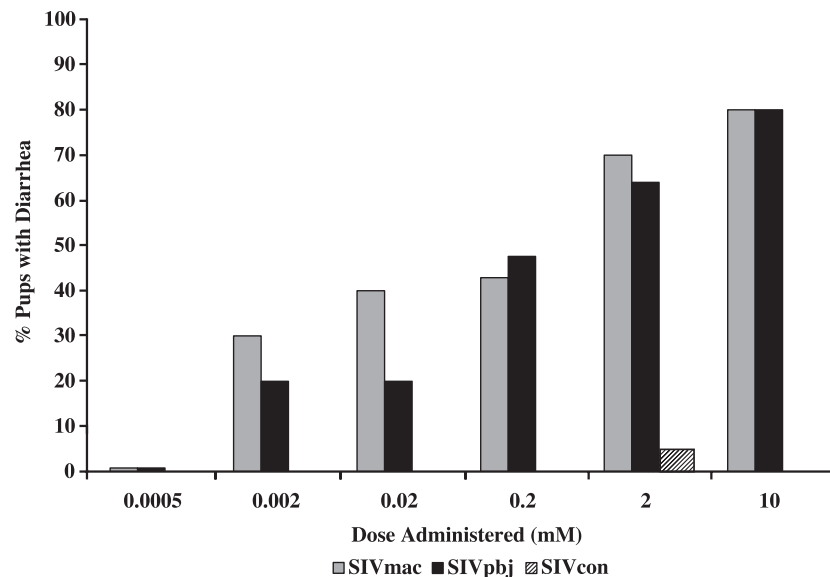
Fig. 1. SIVmac and SIVpbj induced a dose-dependent diarrhea in 6–8-day-old Balb/C mice. Each dose was administered in 50 μl of sterile PBS and was determined to be free of endotoxin. The *x*-axis shows the dose of peptide administered (mM) and the *y*-axis shows the percentage of pups that developed diarrhea. Control pups were inoculated with purified SIVcon (C terminus of SU) or PBS only. The calculated DD_{50} of SIVmac and SIVpbj was 0.15 mM and 0.42 mM, respectively, based on the calculations of Reed and Muench (1938).

would likely yield an excess of viral protein, such as SU, which could complicate the GI alterations by functioning as a viral enterotoxin, similar to SIVmac239 SU, in intact enterocytes.

Several studies show that the third variable domain (V3 loop) of SU is associated with HIV or SIV pathogenesis (Hunter and Swanstrom, 1990; Nelson et al., 2000; Prochiantz, 2000; Sakaida et al., 1998). HIV-1 SU induces $[Ca^{2+}]_i$ mobilization from caffeine-sensitive stores in HT-29 colonic cells that are ablated by V3- or galactosylceramide (GalCer) receptor-specific antibodies (Dayanithi et al., 1995). Based on these data, the authors speculate that the V3 region is enteropathic and contributes to the wasting seen in HIV-infected patients by promoting fluid secretion in the GI tract (Dayanithi et al., 1995). In the current study, we selected analogous regions of SU corresponding to the putative enterotoxic HIV V3 loop sequence from two diverse SIV strains, SIVmac239 and SIVsmmPBj41, and determined if these SIV peptides were enterotoxic. Specifically, peptides were tested for diarrheagenic activity in a mouse model and for induction of IP3 and $[Ca^{2+}]_i$ levels in a human intestinal cell line. To evaluate structure and membrane interactions, we performed circular dichroism (CD) analyses and characterized peptide–membrane interactions.

Results

SIV SU synthetic peptides induced a dose-dependent diarrhea in a mouse model

Each peptide or PBS was independently inoculated IP into 6–8-day-old Balb/C mouse pups and diarrhea was monitored for 24 h. The diarrhea responses to the peptides were specific, as administration of purified SIVcon or the same volume of PBS had little or no effect. Administration of 2 mM SIVcon induced minimal diarrhea in 1/29 (3.4%) of the pups and none of the animals (0/20) administered an equal volume of PBS developed diarrhea (Fig. 1). The incidence of diarrhea ranged from 0% to 80% following administration of 0.5 μM to 10 mM of purified SIVmac or SIVpbj showing a dose response. Based on the calculations of Reed and Muench (1938), the diarrhea dose 50 (DD_{50}) for SIVmac and SIVpbj was 0.15 and 0.42 mM, respectively. These data indicate a lower dose of SIVmac is required for diarrheagenic activity compared to SIVpbj in the mouse model.

For both peptides, the onset of diarrhea was typically within 2 h post administration and continued for up to 8 h, occasionally for up to 24 h. When animals administered with either SIVmac or SIVpbj had severe diarrhea (3 to 4+), they often exhibited lower body temperatures or were lethargic compared to those animals administered the control inoculums. These symptoms are similar to those observed with IP administration of full-length SIV SU

(Swaggerty et al., 2000), HIV-1 SU (Ball and Estes, unpublished data), and $NSP4_{114-135}$ (Ball et al., 1996). Also like the NSP4 enterotoxin, a significantly higher dose of peptide was required when compared to full-length protein to yield equivalent effects, that is, the DD_{50} of SIV SU is 0.13 nmols (Swaggerty et al., 2000).

Histological analysis of SIV SU peptide-treated intestinal loops

Histological evaluations of the tissue and mucosa of the SIVmac-, SIVpbj-, and SIVcon-treated intestinal loops appeared identical (Figs. 2A–C) to the PBS-treated loops (Fig. 2D). Minimal accumulation of neutrophils was observed within and around vessels of the mesentery in both treated and nontreated intestinal tissues. The accumulation
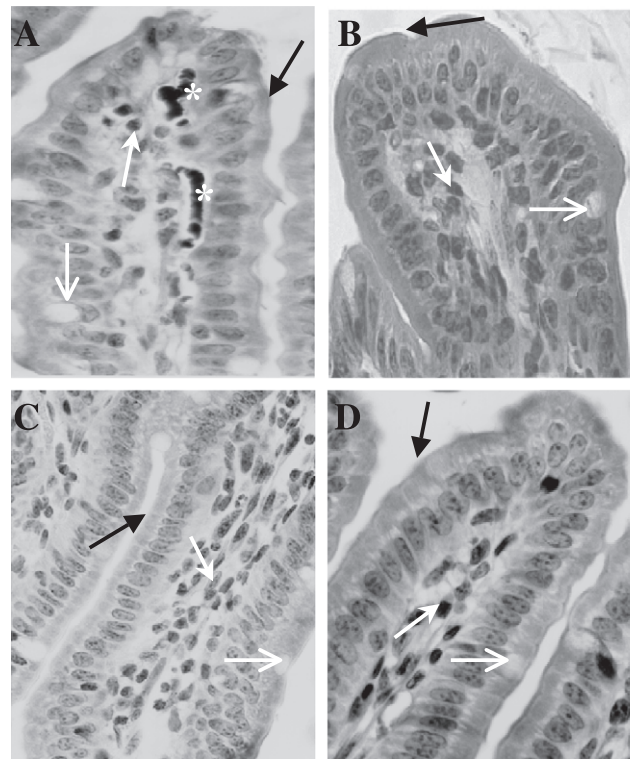

Fig. 2. Hematoxylin and eosin staining of the mucosa from the mouse intestinal loops. (A) SIVmac-treated loop with a normal number of lymphocytes (white, closed arrow) and goblet cells (white, open arrow). The columnar epithelium and microvilli brush-border (black, closed arrow) are unaltered, indicating there are no histological alterations induced by the addition of SIVmac to the intestinal loop. This tissue also has a capillary with red blood cells (white *) that is visible. (B) SIVpbj-treated loop with an equal number of lymphocytes (white, closed arrow) and goblet cells (white, open arrow). The columnar epithelium and the microvilli brush-border remained intact (black, closed arrow). (C) SIVcon-treated intestinal loop with comparable numbers of lymphocytes (white, closed arrow) and goblet cells (white, open arrow). The columnar epithelium and the microvilli brush-border remained intact (black, closed arrow). (D) PBS-treated loop with a normal population of lymphocytes (white, closed arrow) and goblet cells (white, open arrow). The columnar epithelium and the microvilli brush-border are intact (black, closed arrow).

of neutrophils was considered a secondary result due to the manipulation of tying off the loops and subsequent handling during the surgical procedures. No significant lesions or other alterations were observed within the mucosa of any specimens examined from the treatment or control groups. In all tissues examined, the columnar epithelium and microvilli brush border remained intact and there were normal populations of lymphocytes and goblet cells. These data indicate that the secretory response induced by the peptides was not due to cell damage.

SIV SU peptides induced intracellular calcium mobilization in cultured HT-29 cells

$[Ca^{2+}]_i$ mobilization by SIVmac, SIVpbj, or SIVcon was monitored in Fluo-4-loaded HT-29 cells. Addition of 300 μM of each peptide ($n = 4$) increased $[Ca^{2+}]_i$ levels above the basal levels observed in unstimulated cells; however, there were notable differences in the intensity

of the response and the observed patterns (Fig. 3). For comparative purposes, an intensity level of 40 was selected. Fig. 3A shows representative cells from four different experiments in which cells were treated with SIVmac. Seven out of 21 cells (33%) reached fluorescence intensity levels of 40 or greater while 18/22 (82%) of the cells treated with SIVpbj (Fig. 3B) reached levels of 40 or greater. Hence, the SIVpbj peptide was more active in $[Ca^{2+}]_i$ mobilization when compared to SIVmac despite a higher DD_{50}, perhaps due to the use of human cells. Although SIVcon-treated cells reached intensity levels comparable to the SIVmac-treated cells (6/20 or 30%, Fig. 3C), there was a significant difference in the pattern of $[Ca^{2+}]_i$ mobilization indicating a different response. In SIVmac-treated cells that reached intensity levels of 40 or greater, 5/7 (71%) cells had an oscillating calcium response at some point during the experiment; however, the SIVcon-treated cells gradually plateau with no oscillations. Likewise, there was a marked difference in the $[Ca^{2+}]_i$

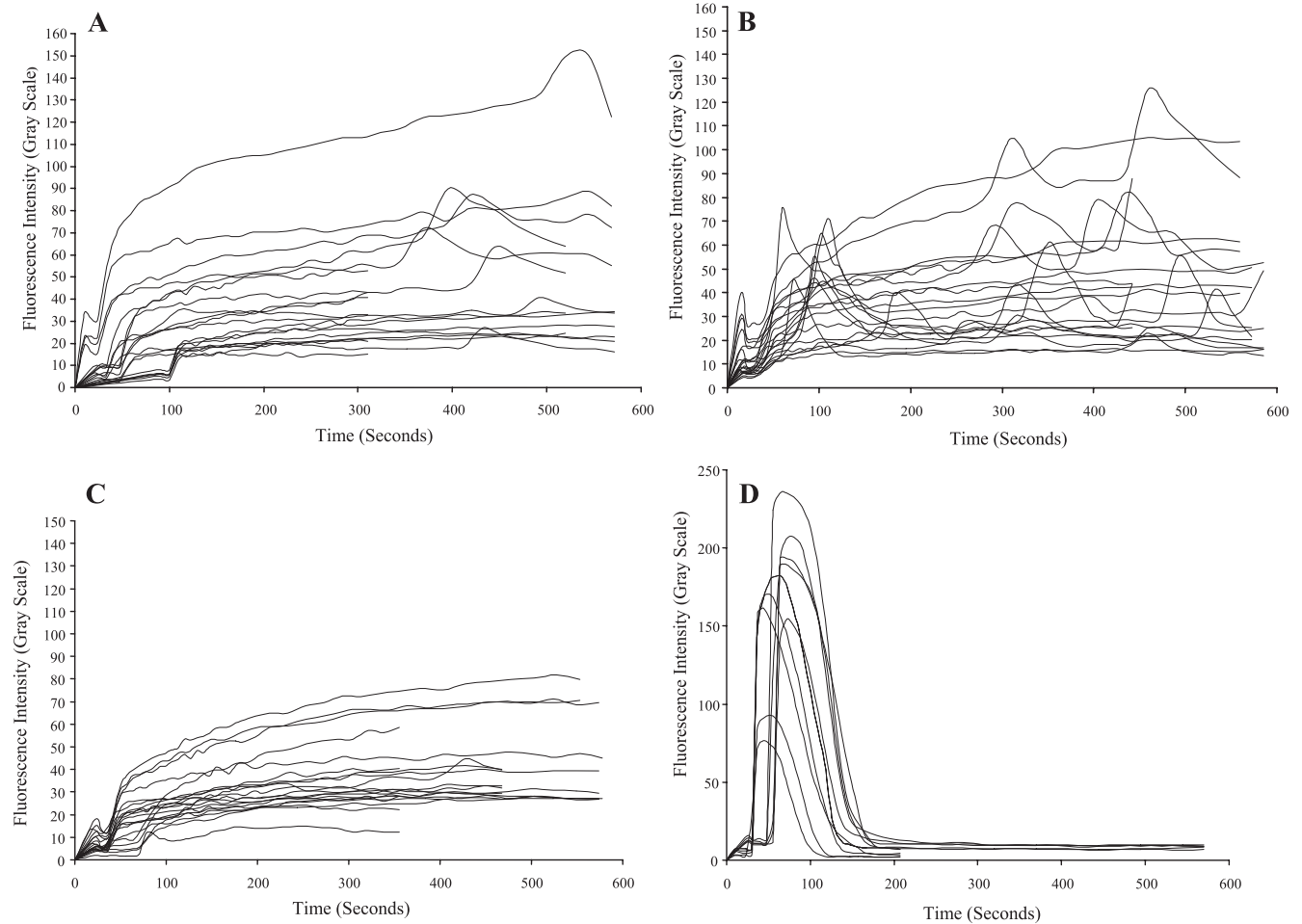Fig. 3. SIV SU peptides mobilized $[Ca^{2+}]_i$ in Fluo-4-loaded HT-29 cells. The x-axis is the time (seconds) and the y-axis is the fluorescence intensity as measured on the gray scale. Representative cell responses are shown from four different experiments. (A) SIVmac-treated cells ($n = 4$). (B) SIVpbj-treated cells ($n = 4$). (C) SIVcon-treated cells ($n = 4$). (D) Neurotensin-treated cells (positive control, $n = 2$).

response pattern in the cells treated with SIVpbj (Fig. 3B). Of the 18 cells that reached intensity levels of 40 or greater, 16/18 (89%) responded with oscillations or multiple oscillations within the same cell. Cells treated with neurotensin responded as previously reported (Swaggerty et al., 2000) and served as positive control (Fig. 3D).

Specificity of the calcium response

Peptide-specific antisera greatly reduced the $[Ca^{2+}]_i$ mobilization induced by SIVmac and SIVpbj, indicating the response is specific. One out of seven cells (14.3%) barely reached fluorescence intensity levels of 40 when treated with SIVmac blocked with 1:10 dilutions of SIV-mac-specific antiserum. When SIVmac was treated with a 1:100 dilution of anti-SIVmac, none of the cells reached intensity levels of 40 or greater. Similarly, only 1/7 (14.3%) or 0/6 cells reached intensity levels of 40 when treated with SIVpbj blocked with 1:10 or 1:100 dilutions of anti-SIVmac, respectively. Treatment with SIVmac antiserum also eliminated the oscillating calcium responses induced by SIVmac and SIVpbj. The effects of anti-SIVcon antiserum on SIVcon-induced calcium response were different. When SIVcon was blocked with a 1:10 dilution of anti-SIVcon, 6/7 (85.7%) of the cells reached intensity levels of 40 with a transient calcium response as opposed to the sustained response induced by untreated SIVcon. Only 1/7 (14.3%) cells reached an intensity level of 40 when SIVcon was blocked with a 1:100 dilution of SIVcon antiserum. Both SIV peptide-specific antisera failed to alter the effects of neurotensin (data not shown), indicating the antibody block was specific.

SIV peptides localized to the plasma membrane and cytoplasm of HT-29 colonic cells

Based on the elevated and sustained calcium responses, we investigated the cellular location of the peptides in HT-29 cells using an immunofluorescence assay (IFA). SIVmac was present on the outside of the plasma membrane (Fig. 4A) as well as in the cytoplasm (Fig. 4B) of the cell. Although HT-29 cells tend to clump, care was taken to indicate single cells (arrows, Figs. 4A–C). SIVcon was also found on the plasma membrane (white open arrow) and in the cytoplasm (white closed arrow) of the cell (Fig. 4C). Cells treated with peptide alone did not fluoresce, nor did cells fluoresce when treated with peptide reacted with species-specific preimmune serum or secondary antibody alone. To ensure that the dye loading procedure did not affect the location of the peptide, an IFA also was conducted with cells that underwent mock dye loading before treatment with SIV-con which showed no difference in the observed staining pattern. Although SIVpbj-specific antibody was not available, SIVpbj would likely cross the membrane, as its molecular weight and amphipathic properties are similar
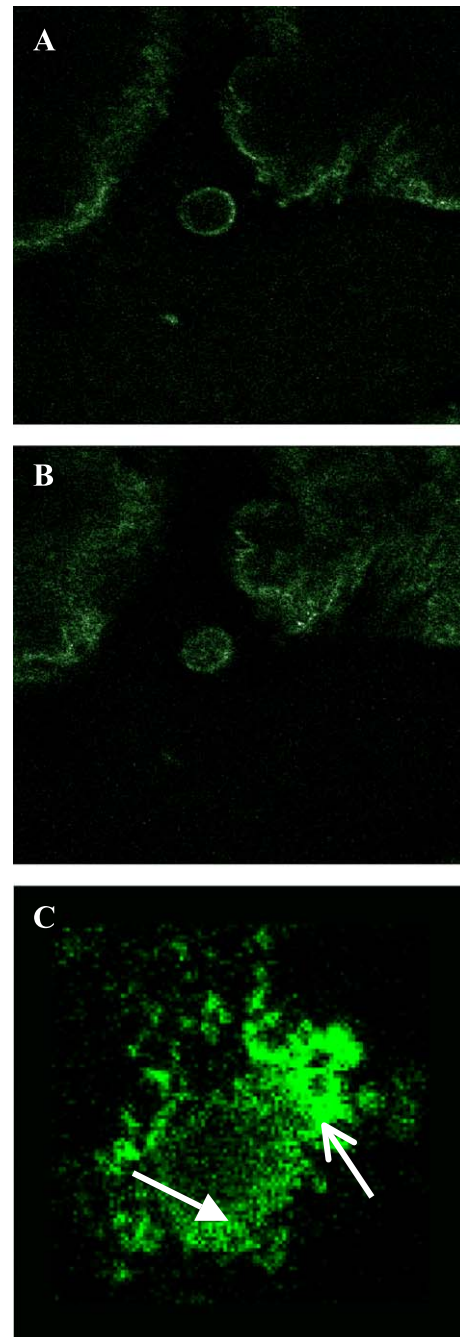
Fig. 4. SIVmac and SIVcon localized to the plasma membrane and in the cytoplasm of HT-29 colonic cells as demonstrated by IFA. (A) HT-29 cells treated with SIVmac, mouse-anti-SIVmac, and FITC-conjugated goat-anti-mouse IgG showing staining on the plasma membrane and (B) in the cytoplasm. (C) HT-29 cells treated with SIVcon, rabbit-anti-SIVcon, and FITC-conjugated goat-anti-rabbit IgG. White closed arrow denotes cytoplasmic staining and the white open arrow is directed at the plasma membrane staining of a neighboring cell.

to SIVmac and SIVcon. Thus, the SU peptides likely act by a different mechanism than the full-length protein to alter calcium homeostasis in the cells when exogenously added to human intestinal cells.

SIV SU peptides increased IP3 in HT-29 colonic cells

A competitive radioreceptor assay was utilized to measure IP3 levels in HT-29 cells treated with SIVmac, SIVpbj, SIVcon, neurotensin, or PBS. SIVmac ($n = 4$) and SIVpbj ($n = 3$) (300 μM) increased IP3 levels 265% and 259% above basal levels, respectively (Fig. 5). Cells treated with 300 μM SIVcon increased levels 153% above background levels observed in buffer-treated cells ($n = 3$). Although the SIVcon peptide increased IP3 levels, the SIVmac and SIVpbj bioactive peptides increased IP3 levels significantly above SIVcon-treated cells ($P < 0.05$). Cells treated with 0.01 μM neurotensin ($n = 4$) responded as previously reported (Swaggerty et al., 2000) and served as positive control (not shown). The significant differences in dose of the SIV peptides compared to neurotensin to induce both the IP3 and calcium responses are likely receptor-related or could be due to (1) the peptide not corresponding to the complete binding domain, (2) reduced innate IP3 stimulation of the SIV peptides, or (3) failure of the SIV peptides to fold in a native conformation.

Secondary structure of the SIV SU peptides promoted in a hydrophobic environment

CD spectra of all three peptides in buffer showed mostly random coil characteristics with a strong negative absorption at approximately 200 nm and very weak negative absorption at 222 nm (Figs. 6–8 panel A, dark circles). These data are not surprising as peptide structure is frequently disordered in an aqueous environment (Lark et al., 1989). Fractions of α-helix calculated for SIVmac, SIVpbj,

and SIVcon were 0.14, 0.17, and 0.15, respectively (Table 1). Thus, SIVpbj with 17% α-helix showed the most innate helical structure.

To evaluate the peptide structure in a more hydrophobic environment, 50% trifluoroethanol (TFE) was utilized. In this hydrophobic solvent, the CD spectra of all three peptides showed typical α-helix characteristics, that is, negative absorption at 222 and 208 nm, and positive absorption at 190 nm (Figs. 6–8 panel A, open circles). Only those peptides with a strong structural propensity demonstrate an ordered structure when placed in an optimal environment (Shoemaker et al., 1985), indicating these SU peptides have a strong α-helical propensity. In 50% TFE the α-helical contents of SIVmac, SIVpbj, and SIVcon were 0.28, 0.32, and 0.31, respectively (Table 1). These data show at least a 2-fold increase in α-helical content in the hydrophobic environment when compared to that in buffer, suggesting a hydrophobic environment, such as membranes, may organize or promote the α-helical structure of the peptides.

SIV SU peptides interact with model membranes of distinct composition and size

Because a hydrophobic environment promoted the SIV peptide helical structure, the peptides were analyzed in the presence of small or large unilamellar vesicles (SUV and LUV, respectively) of different composition. The overall charge, lipid content, and size of the vesicles were altered to directly test if alterations in membrane lipid composition or curvature affected peptide–membrane interactions.
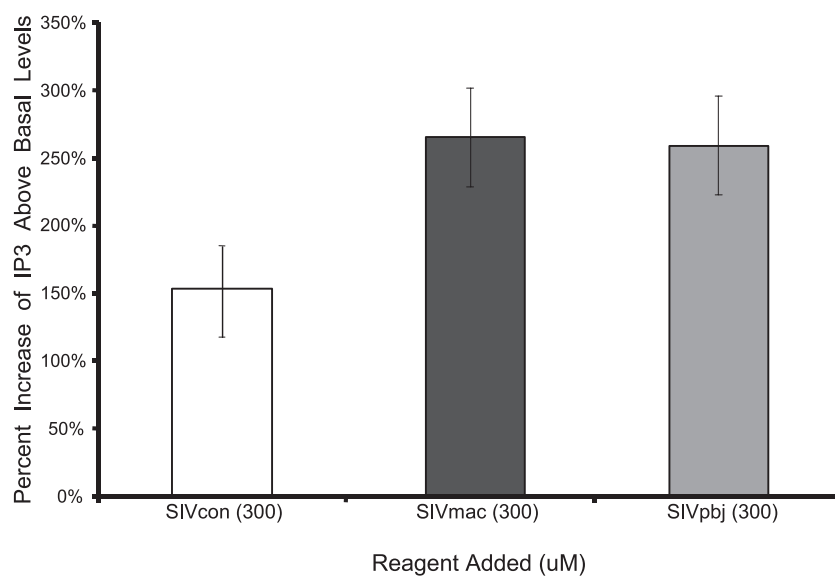

Fig. 5. SIV SU peptides induced an increase in IP3 levels in HT-29 cells. The x-axis is the treatment administered (all were 45 s with $n = 3$ or 4). The y-axis is the percent increase in IP3 levels above background levels in untreated cells. The 300 μM SIVmac and SIVpbj increased IP3 levels 265% and 259%, respectively. SIVcon (300 μM) increased levels 153% above the basal levels.
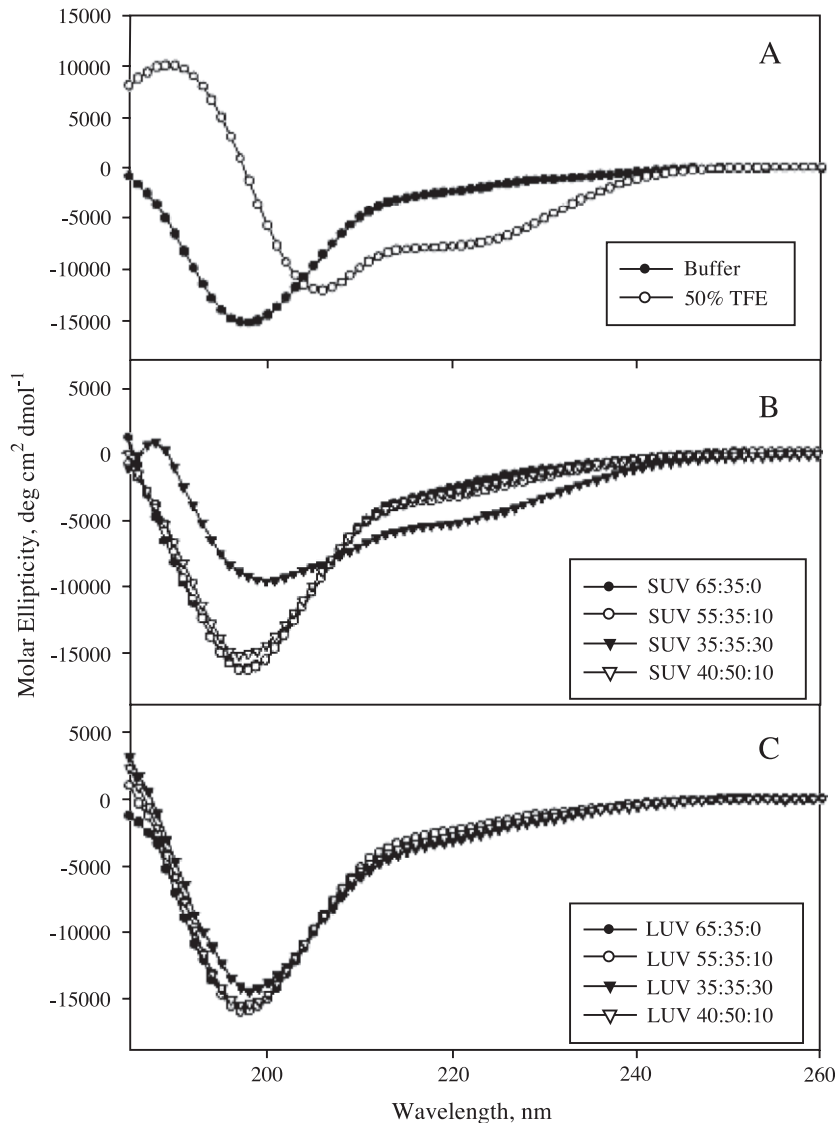
Fig. 6. (Panel A) CD spectra of SIVcon in buffer (dark circles) or 50% TFE (open circles). (Panel B) CD spectra of SIVcon in the presence of SUV. (Panel C) CD spectra of SIVcon in the presence of LUV. In panels B and C, the lipid compositions of the vesicles were as follows: dark circles, POPC/Cholesterol = 65:35; open circles, POPC/Cholesterol/DOPS = 55:35:10; dark triangles, POPC/Cholesterol/DOPS = 35:35:30; open triangles, POPC/Cholesterol/DOPS = 40:50:10. In all the experiments, peptide concentrations were 15 μM, and lipid concentrations of the vesicles were 1 mM.

Effect of charge

In the presence of SUV composed of neutral lipids (1-Palmitoyl-2-oleoyl-sn-glycero-3-phosphocholine [POPC or phosphatidylcholine, PC]/cholesterol molar ratio of 65:35), none of the peptides showed significant changes in CD spectra or calculated α-helical fraction compared to the CD spectra observed in buffer (Figs. 6–8 panel B, dark circles, and Table 1). Because the peptides have a net positive charge, the concentration of negatively charged lipid (1,2-dioleoyl-sn-glycero-3-[phospho-L-serine] [DOPS or phosphatidylserine, PS]) was increased to 10% to evaluate the role of ionic interactions. In the presence of SUV (PC/cholesterol/PS molar ratio of

55:35:10), the SIVpbj and SIVcon peptides showed slightly more negative absorption at 222 nm compared to those in buffer or those in the presence of neutral SUV (Figs. 6–8 panel B, open circles). The α-helical fraction of SIVpbj increased by 9% and SIVcon increased by 18% (Table 1). The changes observed for SIVmac were more profound (Fig. 7, panel B, open circles) as the α-helical fraction increased by 24% when compared to the α-helical content in buffer. When PS was increased 30% in the SUVs, the α-helical fractions further increased to 0.31 for SIVmac, 0.24 for SIVpbj, and 0.22 for SIVcon, a 76%, 24%, and 52% increase compared to buffer alone, respectively. A high radius of curvature in the absence of
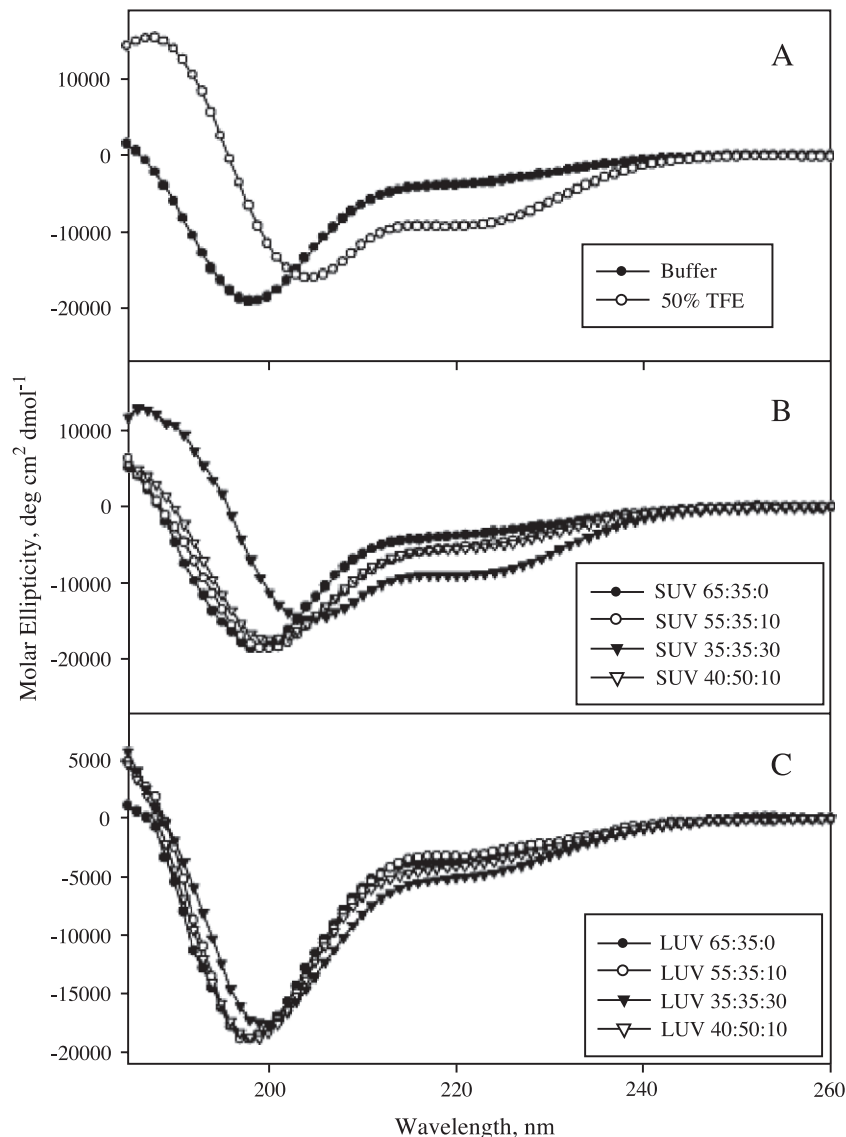
Fig. 7. (Panel A) CD spectra of SIVmac in buffer (dark circles) and 50% TFE (open circles). (Panel B) CD spectra of SIVmac in the presence of SUV. (Panel C) CD spectra of SIVmac in the presence of LUV. In panels B and C, the lipid compositions of the vesicles were as follows: dark circles, POPC/Cholesteol = 65:35; open circles, POPC/Cholesterol/DOPS = 55:35:10; dark triangles, POPC/Cholesterol/DOPS = 35:35:30; open triangles, POPC/Cholesterol/DOPS = 40:50:10. In all the experiments, peptide concentrations were 15 μM, and lipid concentrations of the vesicles were 1 mM.

anionic lipids was insufficient to interact or organize the SIV SU peptides. These data indicate the peptides preferentially interact with negatively charged membranes in the presence of a high radius of curvature similar to NSP4 peptides (Huang et al., 2001).

Effect of cholesterol concentration

To determine the effect(s) of altering the cholesterol content of the SUV on the helical content of the SIV peptides, cholesterol was increased from 35% to 50% (PC/cholesterol/PS molar ratio of 55:35:10 changed to 40:50:10). This alteration yielded no significant changes in any of the CD spectra (Figs. 6–8 panel

B open triangles vs. open circles) or in the calculated α-helical fraction, suggesting the increased cholesterol had no effect on the peptide–membrane interactions (Table 1).

In the presence of LUV (PC/cholesterol molar ratio of 65:35 or PC/cholesterol/PS molar ratio of 55:35:10, or 40:50:10), the CD spectra and calculated α-helical fractions of the peptides remained essentially the same (Table 1, Figs. 6–8 panel C, dark circles, open circles, and open triangles) when compared to peptides in buffer. However, all three peptides did undergo significant changes in CD spectra when the LUV PS content was increased to 30% (Figs. 6–8 panel C, dark
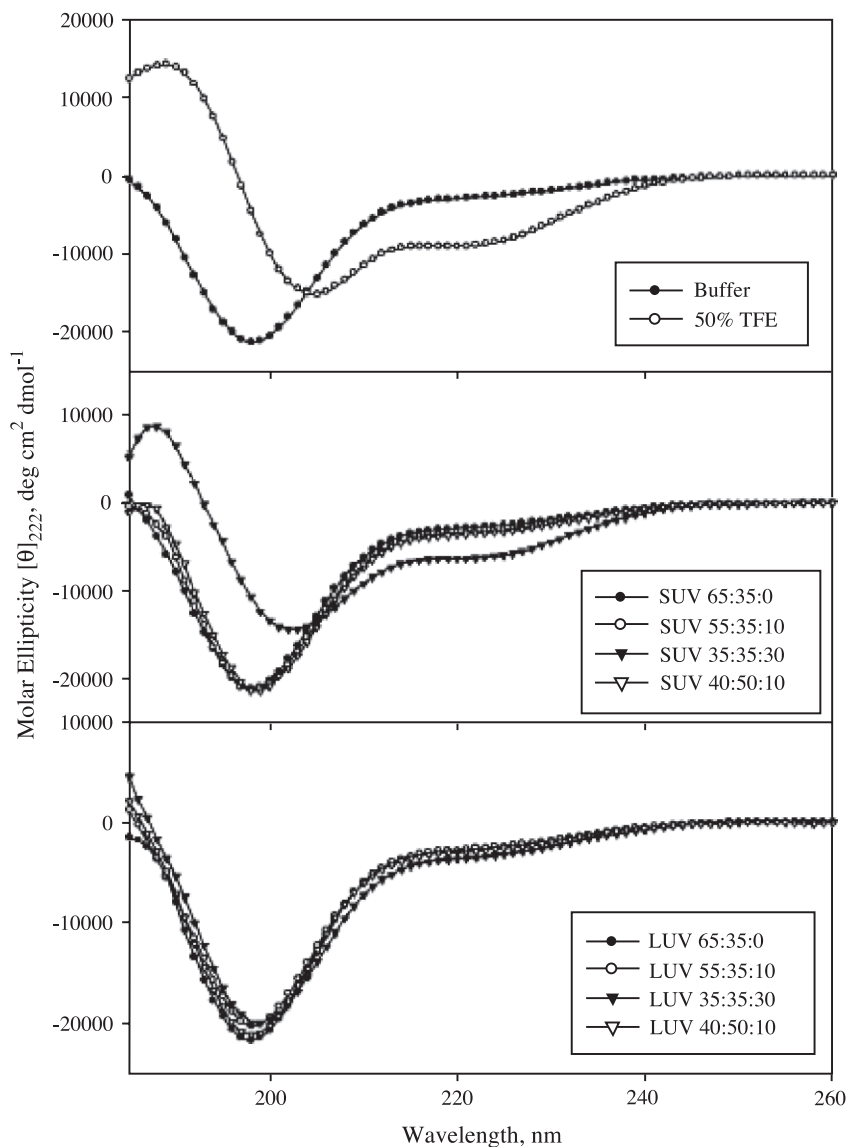
Fig. 8. (Panel A) CD spectra of SIVpbj in buffer (dark circles) and 50% TFE (open circles). (Panel B) CD spectra of SIVpbj in the presence of SUV. (Panel C) CD spectra of SIVpbj in the presence of LUV. In panels B and C, the lipid compositions of the vesicles were as follows: dark circles, POPC/Cholesteol = 65:35; open circles, POPC/Cholesterol/DOPS = 55:35:10; dark triangles, POPC/Cholesterol/DOPS = 35:35:30; open triangles, POPC/Cholesterol/DOPS = 40:50:10. In all the experiments, peptide concentrations were 15 μM, and lipid concentrations of the vesicles were 1 mM.

triangles), albeit lower than that seen with the SUV. The calculated α-helical fraction increased to 0.21 for SIVmac (19% increase), 0.17 for SIVpbj (14% increase), and 0.16 for SIVcon (13% increase) (Table 1). As was seen with the SUVs, SIVmac underwent slightly more secondary structural changes than SIVpbj or SIVcon. To determine if increasing the cholesterol content in the LUV had an effect on peptide–membrane interactions, a molar ratio of 55:35:10 was compared to 40:50:10. Similar to the SUV data, altering the cholesterol content of the LUV did not significantly affect peptide–membrane interactions (Figs. 6–8 panel B vs. panel C, and Table 1).

In summary, all three peptides adopted a mostly random coil structure in buffer and formed 28–32% α-helical structure in 50% TFE. None of the peptides underwent significant secondary structural changes in the presence of neutral vesicles (SUV or LUV), whereas the peptides showed significant ($P < 0.01$) increases in α-helical content in the presence of SUV composed of 10% and 30% PS or LUV with 30% PS. Overall, increasing vesicle PS content promoted peptide interactions, whereas increasing the cholesterol content had no effect. These data indicate the peptides are more organized in the presence of anionic phospholipids. The peptides underwent more secondary structural changes when reacted with the SUVs than with

Table 1
Calculated α-helical fraction of peptides

	Fraction of α-helix (Mean ± SE, n = 4)		
	SIVcon	SIVmac	SIVpbj
Buffer	0.141 ± 0.003	0.174 ± 0.002	0.152 ± 0.001
50% TFE	**0.279 ± 0.003	**0.317 ± 0.003	**0.306 ± 0.001
SUV 65:35:0[a]	0.147 ± 0.002	0.173 ± 0.004	0.151 ± 0.0004
55:35:10[a]	**0.167 ± 0.002	**0.215 ± 0.001	**0.165 ± 0.001
35:35:30[a]	**0.215 ± 0.001	**0.307 ± 0.004	**0.239 ± 0.002
40:50:10[a]	**0.156 ± 0.001	**0.219 ± 0.002	**0.169 ± 0.003
LUV 65:35:0[a]	0.145 ± 0.004	0.167 ± 0.005	0.155 ± 0.001
55:35:10[a]	0.143 ± 0.005	0.162 ± 0.008	0.152 ± 0.002
35:35:30[a]	**0.160 ± 0.0001	**0.207 ± 0.001	**0.174 ± 0.001
40:50:10[a]	0.151 ± 0.001	0.182 ± 0.0002	0.158 ± 0.0004

[a] Lipid composition of the vesicles, POPC/Cholesterol/DOPS.
** Significantly different from those of peptide in buffer, $P < 0.01$.

the LUVs of the same lipid composition, suggesting a preference for membranes with a high radius of curvature.

Discussion

The use of synthetic peptides to dissect mechanisms of viral pathogenesis is well established. Peptide chemistry was utilized to dissect the functionally active enterotoxic domain of the first described viral enterotoxin, rotavirus NSP4 (Ball et al., 1996). $NSP4_{(114-135)}$, a 22 amino acid residue peptide, maintains the enterotoxic properties associated with the full-length NSP4 protein, while other amphipathic peptides or single amino acid mutants of $NSP4_{(114-135)}$ do not induce disease (Ball et al., 1996). Additionally, the use of synthetic peptides has aided in the understanding of lentivirus pathogenesis, particularly in regard to HIV-1 and -2 neutralizing epitopes (Kliger et al., 2001; Misumi et al., 2003; Sharon et al., 2002) and coreceptor usage (Barbouche et al., 2000; Cormier et al., 2000; Dettin et al., 2002; Prochiantz, 2000; Sakaida et al., 1998). Peptides corresponding to the V3 loop of a T-tropic HIV-1 strain show V3 interacts with its coreceptor independent of the V1 or V2 components of SU or cellular CD4 (Sakaida et al., 1998).

The aim of this study was to localize and further characterize the enterotoxic region(s) of two distinct SIV strains, SIVmac239 and SIVsmmPBj14, and to determine if there is a common enteropathic region within the SIV SU glycoprotein. Because the original work was performed with an SU recombinant protein generated from the SIVmac239 strain, it was important to examine the enterotoxic activity of SU peptides from the SIVmac239 sequence (Swaggerty et al., 2000). The SIVsmmPBj14 SU sequence was selected because of reports of acute GI dysfunction, disease, and death in monkeys within 6–10 days post infection (Fultz et al., 1989; Lewis et al., 1992). Although SIVsmmPBj14 is known to damage the intestinal architecture resulting in malabsorption, it remains unclear if SIVsmmPBj14 SU also contains enterotoxic activity that could contribute to the GI disease. In

this study, (1) both SIVmac and SIVpbj peptides induced a dose-dependent diarrheal response in a mouse pup model; (2) neither peptide altered the histology within intestinal loops; (3) both peptides mobilized $[Ca^{2+}]_i$ and (4) increased IP3 levels in cultured HT-29 cells; (5) both peptides demonstrated a dominant random coil secondary structure that increased in α-helical content in a hydrophobic environment; and (6) both peptides preferentially interacted with cholesterol-containing model membranes rich in negatively charged lipids, and with high membrane curvature.

Both SIVmac and SIVpbj induced diarrhea in our mouse model; however, SIVmac was 2.8-fold more active than SIVpbj (DD_{50} of 0.15 and 0.42 mM, respectively). It is possible that the selected sequence for SIVpbj peptide synthesis was not ideal for enterotoxic activity or the neonatal mouse intestines may lack the necessary receptor(s) for optimal enterotoxic activity. Alternatively, enterotoxic activity may not significantly contribute to SIVpbj14-induced diarrheal disease. Data obtained from the negative control peptide, SIVcon, indicate that the C-terminus does not contribute to diarrhea induction and is likely not part of the active enterotoxic domain. However, the C-terminal region of SU may be important in the overall enterotoxic activity by contributing to the structure of the protein and interacting with signaling molecules as supported by this study wherein both IP3 and $[Ca^{2+}]_i$ levels are increased by SIVcon-treated HT-29 cells.

The presence of a viral enterotoxin in SIV or HIV offers one explanation for the devastating GI dysfunction or wasting of AIDS or SAIDS (Ehrenpreis et al., 1992; Heise et al., 1993) when a known causative agent cannot be identified. This study does not discount those instances in which the GI disorders are associated with an identifiable enteric pathogen or intestinal disruption, such as that seen following SIVsmmPBj14 infection (Farthing, 2000; Fultz and Zack, 1994; Fultz et al., 1989; Lewis et al., 1992). However, the data do support the presence of an SIV SU enterotoxic domain that may contribute to the wasting syndrome of HIV or SIV infections. No histological alterations were noted in any of the treated loops, further indicating an enterotoxic pathway rather than malabsorption. Both bioactive peptides increased IP3 levels 1.7-fold more than SIVcon, in agreement with the HIV data showing the V3 loop region contains enterotoxic activity (Dayanithi et al., 1995).

The calcium responses elicited by the SIV peptides were distinct from the full-length SU response (Swaggerty et al., 2000) in that it was sustained rather than transient and had clear oscillations. The SIV peptide responses were similar to that observed when HIV-1 Tat was added to neurons with $[Ca^{2+}]_i$ levels rarely returning to baseline after peptide addition and undergoing fluxes representative of calcium oscillations or waves (Haughey et al., 1999). The observed calcium response was typically initiated within seconds after the addition of the SIV peptides.

This rapid response is significant given calcium response times of a few seconds are generally IP3-mediated (Rooney and Thomas, 1993; Sanderson et al., 1990, 1994). The elevated IP3 levels in the SIV peptide-treated intestinal cells further support an IP3-mediated calcium response. However, there are alternative explanations. The sustained calcium response could be the result of store-operated channels in which a calcium-induced calcium release produces a wave that passes from one cell to the next through gap junctions (Sanderson et al., 1990). Transfection of COS-1 cells with a Golgi-specific Ca^{2+} pump reveals oscillations also resulting from calcium release from non-ER calcium store(s) (Missiaen et al., 2001). It has been shown in primary rat mammatropes that the oscillation pattern of a single cell could change from one distinct pattern to another over time (Shorte et al., 2000; Villalobos et al., 1998). Clearly, additional studies are required to define the mechanism(s) of calcium oscillation patterns observed with the SIV SU peptides.

SIVmac, SIVpbj, and SIVcon assumed a mostly randomly coiled structure in aqueous buffer (14–17% α helix) that significantly increased in α-helical content (28–32%) when exposed to a hydrophobic environment (TFE), an environment known to favor secondary structure in peptides by promoting intramolecular hydrogen bonding. $NSP4_{114-135}$ shows the same trend with 37% α-helical structure in buffer that increases to 91% in the presence of TFE (Huang et al., 2001). In addition, the SIV and NSP4 enterotoxic peptides preferentially interacted with defined membrane lipid domains with a high radius of curvature and rich in anionic phospholipids (Huang et al., 2001). The radius of curvature increases as the diameter of the lipid vesicle decreases, such that SUV with an average diameter of 25 nm has a high radius of curvature with an outer to inner membrane lipid mole ratio of 2.2:1 (Cullis et al., 1996). In contrast, the mean diameter of the LUV is larger, the radius of curvature decreases, and the distribution of lipid between the outer and inner membranes is close to 1:1. Hence, the increased helical content of the SIV peptides with vesicles of a high radius of curvature may be due to the increased exposure of anionic lipids on the outer leaflet.

The NSP4 peptide preferentially bound cholesterol-rich vesicles, while SIV peptide–membrane interaction(s) appeared to require cholesterol, but additional molar concentrations above 35% failed to enhance membrane interactions. The intestinal microvillus is enriched in the number of membranes that are highly curved (Boffelli et al., 1997; Lipka et al., 1995), which may enhance infection and activity of the virus and the enterotoxic protein. Additionally, cholesterol-rich rafts have been shown to stabilize HIV-1 and SIV integrity and infectivity (Graham et al., 2003). Consequently, the SIV SU peptides may interact with lipid rafts on the cell surface. This correlates with a study by Nehete et al. (2002), which shows HIV V3 loop peptides specifically bind host cell glycosphingolipids that may be a critical post-CD4-binding event.

We have identified an enterotoxic domain within SIV SU of two diverse strains, SIVsmmPBj14 and SIVmac239, which corresponds to the putative HIV-1 SU enteropathic domain overlapping the V3 loop. These data suggest that full-length SU is not essential for activity and that these two strains of SIV contain an enteropathic region, as seen with HIV-1. In this study, the mouse provided a convenient, small animal model to readily evaluate the presence of and differences in enterotoxic activity of the SIV peptides. Additional studies examining the SU glycoprotein or synthetic peptides of other lentiviruses are needed to determine if the enterotoxic nature of SU is a common lentivirus virulence factor. Finally, these data, together with additional studies of the enterotoxic properties of HIV or SIV, may direct future studies in the development of therapeutics against HIV- or SIV-induced GI dysfunction.

Materials and methods

Selection of peptides

Synthetic peptide sequences were selected from algorithms that predict surface potential (Parker et al., 1986), turn potential, and amphipathic structure (Margolit et al., 1987). We selected peptide sequences calculated to be amphipathic, hydrophilic, and overlapped the V3 region as the putative enteropathic peptides. Peptide selection was limited to the V3 loop region of SIV SU because it has been shown that HIV-1 V3 alters calcium homeostasis and could be enteropathic (Dayanithi et al., 1995). The control peptide was selected because of its predicted amphipathic structure, similar charge to the V3 peptides, centrally located tyrosine (Y) residue, and the SU C-terminal location (from the same protein). Note that charge, amphipathic character, and a centrally located Y were shown to be critical to the NSP4 peptide enterotoxic activity (Ball et al., 1996). Likewise, the control Nowalk virus peptide used in the NSP4 study was amphipathic, highly charged, and contained a central Y residue, yet was not active in any of the assays. Likewise, several of our assays were tested with the Norwalk virus control peptide to ensure the assays were functioning similar to what was seen in the original NSP4 study (data not shown).

Peptide synthesis, purification, and characterization

SIVmac239 (352–382) (DAIKEVKQTIVKH-PR*Y*TGTNNTDKINLTAPG) (GenBank ID# 135474), SIVsmmPBj41 (360–390) (KAIQEVKETLVKH-PR*Y*TGTNKTEQIKLTAPG) (Dewhurst et al., 1992), and SIVmac239 (496–525) (non-V3 loop control) (DYKL-VEITPIGLAPTDVKR*Y*TTGGTSRNKR) were synthesized

on a Millipore 9050 Plus automated PepSynthesizer (Millipore Corporation, Marlborough, MA) using 9-fluorenylmethylcarbonyl (Fmoc) chemistry following standard activation and deprotection protocols. The peptides are called SIVmac, SIVpbj, and SIVcon, respectively. All chemicals for peptide syntheses were obtained from PerSeptive Biosystems (Framingham, MA). Following cleavage of the peptide from the solid support, 90% trifluoroacetic acid (TFA), 5% thioanisole, 3% ethanedithiol, 2% anisole, and the peptide–resin mixture were filtered through a Buchner funnel (20C fritted disc) into a polypropylene tube containing ice-cold anhydrous ethyl ether. The precipitated peptides were pelleted ($225 \times g$) for 3–5 min, extracted with ether and pelleted three more times, dried under compressed nitrogen gas, solubilized in 10% glacial acetic acid, and lyophilized (Dura Dry MP Microprocessor Controlled Freeze Dryer, FTS Systems, Inc., Stone Ridge, NY). The crude peptides were purified by gravimetric gel filtration chromatography (Sephadex G-25M, Sigma) monitored at 220 nm (ISCO model 229 UV–VIS detector, ISCO, Lincoln, NE) and analyzed by reverse-phase HPLC (Beckman System Gold, Fullerton, CA) on a C4 analytical column (Waters C4 Delta Pak column, Milford, MA). Purified peptides were evaluated by MALDI/Time of flight mass spectroscopy (Laboratory for Biological Mass Spectroscopy, Department of Chemistry, Texas A&M University). Peptide fractions with the correct theoretical mass were used in this study (SIVmac = 3424, SIVpbj = 3478, SIVcon = 3350).

Endotoxin assay

Purified peptides and phosphate-buffered saline (PBS) were assayed for the presence of endotoxin using the *Limulus* Amebocyte Lysate (LAL) test (Associates of Cape Cod, Inc., Falmouth, MA) in endotoxin-free flint (soda lime) glass tubes according to the manufacturer's protocol. A value of 0.5 EU/ml or less was considered acceptable for use in our experiments.

Mouse inoculation and diarrhea scoring

Balb/C mice were acquired from Harlan Sprague–Dawley, Inc. (Indianapolis, IN) or Charles River Laboratories (Wilmington, MA) and housed at Texas A&M University Laboratory Animal Resources and Research Facility. Purified SIVpbj, SIVmac, and SIVcon peptides were diluted in 50 µl sterile, endotoxin-free PBS and were injected intraperitoneally (IP) into 6–8-day-old pups using a 30-G needle. To determine if the diarrheal response was dose-dependent, 0.0005–10 mM of SIVpbj and SIVmac were administered to 86 and 57 pups, respectively. Pups were administered 2 mM SIVcon ($n = 29$) or PBS ($n = 17$), which served as the negative controls. Following injection, the pups were monitored for diarrhea as previously described and scored by one person

on a scale of 1 to 4 (Ball et al., 1996; Swaggerty et al., 2000).

Histological analysis

Peptides were surgically introduced into mouse intestinal loops as previously described (Swaggerty et al., 2000). Eleven animals were administered 50 µl SIVmac (2 mM) dissolved in sterile, endotoxin-free PBS while six animals were given the same concentration and volume of SIVpbj. Twenty-one animals received 50 µl SIVcon (2 mM) or PBS and served as the negative controls. SIV peptide-treated loops were examined for histological changes as previously described (Swaggerty et al., 2000). The intestinal loops were fixed in neutral buffered formalin for 24 h. An unmanipulated segment of intestine not included in the intestinal loop from each animal was removed to serve as a control. Representative sections of the loop were processed, embedded, sectioned, and stained with instant hematoxylin (Shandon, Pittsburgh, PA) and eosin (Sigma) as per routine methodology for microscopic examination.

Loading HT-29 cells with Fluo-4 for calcium imaging

HT-29 cells, human colon adenocarcinoma (ATCC, Rockville, MD), were seeded at 1.0×10^4 cell/ml into LAB-TEK 4-well chamber slides with coverglass slides (0.75 ml/well) (Nalge Nunc International Corporation, Naperville, IL) and allowed to grow for 12–16 h at 37 °C, 5% CO_2. Cells were loaded with Fluo-4 (Molecular Probes, Eugene, OR) in 500 µl physiological calcium-free buffer (PCFB [150 mM NaCl, 5 mM KCl, 10 mM glucose, 20 mM HEPES, 1 mM $MgCl$]) (Steinberg et al., 1987) containing 3% FBS and 0.04% Pluronic F-127 (Sigma) as previously described (Swaggerty et al., 2000). SIVmac, SIVpbj, SIVcon (300 µM final concentration), or neurotensin (0.005 µM final concentration) was diluted in 200 µl PCFB and added to the cells immediately before analysis and data collection.

Laser scanning confocal microscopy (LSCM)

The calcium imaging studies were performed on a MRC-1024 laser scanning confocal microscopy (LSCM) imaging system controlled by LaserSharp software (Bio-Rad, Laboratories, Hercules, CA). A region of 10–20 cells was randomly selected, the median section along the z-axis of the cells was viewed, and the calcium kinetics monitored by acquiring images at 10-s intervals and calculating the average pixel intensity using the Time Course Software (Bio-Rad Laboratories).

LSCM was also utilized to determine if the peptides penetrated the cell membrane or if they were bound and localized to the outside of the cell. HT-29 cells were grown to 80% confluency in LAB-TEK 4-well chambered coverglass slides, treated with 300 µM SIVmac or SIVcon for 10

min at 25 °C, and an immunofluorescence assay (IFA) was performed. The peptides were removed and the cells rinsed with PBS and fixed and permeabilized with ice-cold methanol/acetone (1:1) for 10 min at −20 °C. The slides were dried, rehydrated with PBS, and then incubated in blocking buffer (3% dry milk in PBS with 0.02% Triton X-100) for 1 h at 25 °C. Primary antibodies (rabbit-anti-SIVcon, mouse-anti-SIVmac, normal rabbit, or normal mouse sera) prepared in 1% dry milk in PBS were added to the cells and incubated for 1 h at 25 °C. Following four washes with 0.5% dry milk in PBS, secondary antibodies (anti-rabbit IgG, H and L chain (goat)-FITC [Calbiochem-Novabiochem Corporation, San Diego, CA] or anti-mouse IgG (goat)-FITC [Jackson Immuno Research Laboratories, West Grove, PA]) prepared in 1% dry milk were added to the cells and incubated for 30 min at 25 °C, washed, then viewed (488 line, 3–10% laser power, 522/DF35 filter).

Specificity of the calcium response

SIVmac, SIVpbj, and SIVcon peptides (2 mM) were prepared in PCFB. The peptides were incubated for 1 h at 25 °C with 1:10 or 1:100 dilutions of corresponding antibodies. Because SIVmac and SIVpbj shared highly homologous sequences (74% identity), they were both blocked with mouse-anti-SIVmac antiserum; SIVcon was blocked with rabbit-anti-SIVcon antiserum. Both antisera were mixed with 10 nM neurotensin at a 1:10 dilution to control for nonspecific inactivation. After the HT-29 cells were loaded with Fluo-4, 200 μl of antisera-treated SIVmac, SIVpbj, SIVcon (1 mM final concentration) or neurotensin (0.005 μM final concentration) was diluted in 200 μl PCFB, added to the cells, and evaluated for calcium kinetics.

Inositol 1,4,5-triphosphte (IP3) measurements

To determine if the mechanism of peptide-induced $[Ca^{2+}]_i$ mobilization is similar to full-length SU, the IP3 assay was performed as previously described (Swaggerty et al., 2000). HT-29 cells were either mock-treated or treated with 300 μM SIVmac, SIVpbj, SIVcon, or 0.01 μM neurotensin prepared in Na-HEPES-buffered saline (140 mM NaCl, 4.7 mM KCl, 1.13 mM MgCl$_2$, 10 mM HEPES, 10 mM glucose, 1 mM CaCl$_2$) for 45 s. Samples were assayed for IP3 by a competitive radioreceptor assay (Amersham Pharmacia Biotech [kit number TRK1000], Piscataway, NJ) according to the manufacturer's instructions. Radioactivity in 5 ml scintillation fluid (CytoScint (ICN Biomedicals, Inc. Irvine, CA) was measured for 4 min using a 1600 TR Tri-Carb liquid scintillation analyzer (Packard Instrument Company, Downers Grove, IL).

Preparation of small unilamellar vesicles (SUV)

The interactions of the enterotoxic peptides with specific lipid domains were examined using small and large uni-lamellar vesicles (SUV and LUV, respectively) composed of the phospholipids 1-Palmitoyl-2-oleoyl-*sn*-glycero-3-phosphocholine (POPC or PC) and 1,2-dioleoyl-*sn*-glycero-3-[phospho-L-serine] (DOPS or PS) and cholesterol (Avanti Polar Lipids, Alabaster, AL). SUVs composed of varying molar ratios of PC/cholesterol/PS (molar ratio 65:35:0, 55:35:10, 35:35:30, 40:50:10) were prepared by sonication and analyzed as previously described (Hapala et al., 1994; Schroeder et al., 1987). Solvents were removed under N$_2$ with constant rotation and were subsequently dried under vacuum for a minimum of 4 h. The sample was diluted in prefiltered 3-[*N*-morpholino] propane-sulfonic acid buffer (MOPS, 10 mM), pH 7.4, vortexed, bath sonicated, and vortexed again. The resultant multilamellar membrane suspension was sonicated with a microprobe (Sonic Dismembrator Model 550, Fisher) under N$_2$ at 4 °C at energy level 4 using 1-min pauses after every 2 min of sonication to prevent overheating. The sonicated solution was centrifuged using a 40 Ti rotor (Beckman) at 35 K for 4 h to remove any multilamellar vesicles and titanium debris left from the sonicator probe. This protocol was shown to produce vesicles with a diameter of 20–30 nm by photon correlation spectroscopy and with a high radius of curvature (Huang et al., 1999, 2001). The lipid concentration of the final SUV solution was determined by a standard phosphate assay (Ames, 1968). UV absorbance was recorded at 660 nm and the concentration of the phospholipids in the SUV was calculated using a standard curve of the UV absorbance plotted against a known concentration of phospholipid.

Preparation of large unilamellar vesicles (LUV)

For comparison, large unilamellar vesicles (LUV) were prepared by extrusion through polycarbonate membranes. All procedures were the same as described for the preparation of the SUV, except sonication was omitted. Instead, the lipid suspension was freeze–thawed five times and extruded 21 times (back and forth) through double layers of 0.1 μm polycarbonate membranes in a mini-extruder (Avanti Polar Lipids) which produces vesicles with a diameter of 100–120 nm by photon correlation spectroscopy (Huang et al., 1999, 2001) and a small radius of curvature.

Secondary structure estimation by circular dichroism (CD)

Secondary structures of the peptides were determined in aqueous buffer and trifluoroethanol (TFE), a hydrophobic solvent. To determine if the SIV SU peptides interact with caveolae-like membranes, similar to the NSP4 enterotoxic peptide, interactions of the three SIV peptides with SUV and LUV were determined by circular dichroism (CD) following a modified procedure (Huang et al., 2001; Stolowich et al., 1997). The concentration of the peptide solution was determined by amino acid analysis (Protein Chemistry Core Laboratory, Texas A&M University). The

15-µM peptide solution in the absence or presence of 1 mM lipid vesicles, buffer alone (10 mM phosphate buffer, pH 7.4), or lipid vesicles without peptide was examined by CD. CD spectra were obtained at 25 °C in a 1 mm circular quartz cell and a Model J-710 Spectropolarimeter (JASCO Inc, Easton, MD). Each CD spectrum was from 185 to 260 nm with a step resolution of 1 nm, speed of 50 nm/min, response of 1 s, bandwidth of 2.0 nm, and sensitivity of 10 mdeg. Data from 10 scans were averaged, background subtracted, and converted to mean residue molar ellipticity $[\theta]$ (deg cm^2/dmol).

The equation $\theta_{222} = (_h - i\kappa / N)[\theta_{h\ 222\infty}]$ was used to estimate the percent helix for each peptide with θ_{222} as the mean residue molar ellipticity at 222 nm, $_h$ as the fraction in α-helical form, i as the number of helices, κ as a wavelength-specific constant with a value of 2.6 at 222 nm, N as the number of residues in the peptide, and $\theta_{h\ 222\infty}$ represents the molar ellipticity for a helix of infinite length at 222 nm (i.e., −39500 deg cm^2/dmol) (Chang et al., 1978; Chen et al., 1974).

Acknowledgments

References

Alexander, L., Du, Z., Howe, A.Y.M., Czajak, S., Desrosiers, R.C., 1999. Induction of AIDS in rhesus monkeys by a recombinant simian immunodeficiency virus expressing nef of human immunodeficiency virus type 1. J. Virol. 73, 5814–5825.

Ames, B.N., 1968. Assay of inorganic phosphate, total phosphate and phosphatases. Methods Enzymol. 8, 115–118.

Ball, J.M., Tian, P., Zeng, C.Q.Y., Morris, A.P., Estes, M.K., 1996. Age-dependent diarrhea induced by a rotaviral nonstructural glycoprotein. Science 272, 101–104.

Barbouche, R., Papandreou, M.J., Miquelis, R., Guieu, R., Fenouillet, E., 2000. Relationships between the anti-HIV V(3)-derived peptide SPC(3) and lymphocyte membrane properties involved in virus entry: SPC(3) interferes with CXCR(4). FEMS Letters 183, 235–240.

Boffelli, D., Weber, F.E., Compassi, S., Werder, M., Schulthess, G., Hauser, H., 1997. Reconstitution and further characterization of the cholesterol transport activity of the small-intestinal brush border membrane. Biochemistry 36, 10784–10792.

Chang, C.T., Wu, C.-S.C., Yang, J.T., 1978. Circular dichroic analysis of protein conformation: inclusion of the beta turns. Anal. Biochem. 91, 13–31.

Chen, Y.-H., Yang, J.T., Chau, K.H., 1974. Determination of the helix and beta form of proteins in aqueous solution by circular dichroism. Biochemistry 13, 3350–3359.

Cormier, E.G., Persuh, M., Thompson, D.A., Lin, S.W., Sakmar, T.P., Olson, W.C., Dragic, T., 2000. Specific interaction of CCR5 amino-terminal domain peptides containing sulfotyrosines with HIV-1 envelope glycoprotein gp120. PNAS, USA 97, 5762–5767.

Cullis, P.R., Fenske, D.B., Hughes, S.H., 1996. Biochemistry of Lipids, Lipoproteins and Membranes. Elsevier, New York.

Dayanithi, G., Yahi, N., Baghdiguian, S., Fantini, J., 1995. Intracellular calcium release induced by human immunodeficiency virus type 1 (HIV-1) surface envelope glycoprotein in human intestinal epithelial cells: a putative mechanism for HIV-1 enteropathy. Cell Calcium 18, 9–18.

Dettin, M., Scarinci, C., Pasquato, A., DiBello, C., 2002. Synthetic peptides for study of human immunodeficiency virus infection. Applied Biochem. and Biotech. 102–103, 41–47.

Dewhurst, S., Embretson, J.E., Fultz, P.N., Mullins, J.I., 1992. Molecular clones from a non-acutely pathogenic derivative of SIVsmmPBj14: characterization and comparison to acutely pathogenic clones. AIDS Res. Hum. Retroviruses 8, 1179–1187.

Du, Z., Lang, S.M., Sasseville, V.G., Lackner, A.A., Ilyinskii, P.O., Daniel, M.D., Jung, J.U., Desrosiers, R.C., 1995. Identification of a nef allele that causes lymphocyte activation and acute disease in macaque monkeys. Cell 82, 665–674.

Ehrenpreis, E.D., Ganger, D.R., Kochvar, G.T., Patterson, B.K., Craig, R.M., 1992. D-xylose malabsorption: characteristic finding in patients with the AIDS wasting syndrome and chronic diarrhea. J. Acquired Immune Defic. Syndr. 5, 1047–1050.

Farthing, M.J.G., 2000. Enterotoxin and the enteric nervous system—a fatal attraction. Int. J. Microbiol. 290, 491–496.

Fultz, P.N., 1994. SIVsmmPBj14: an atypical lentivirus. In: Letvin, N.L., Desrosiers, R.C. (Eds.), Simian Immunodeficiency Virus, vol. 188. Springer-Verlag, Berlin, pp. 65–76.

Fultz, P.N., Zack, P.M., 1994. Unique lentivirus–host interactions: SIVsmmPBj14 infection of macaques. Virus Res. 32, 205–225.

Fultz, P.N., McClure, H.M., Anderson, D.C., Switzer, W.M., 1989. Identification and biological characterization of an acutely lethal variant of simian immunodeficiency virus from sooty mangabeys (SIV/SMM). AIDS Res. Hum. Retroviruses 5, 397–409.

Graham, D.R.M., Chertova, E., Hilburn, J.M., Arthur, L.O., Hildreth, J.E.K., 2003. Cholesterol depletion of human immunodeficiency virus type 1 and simian immunodeficiency virus with β-cyclodextrin inactivates and permeabilizes the virions: evidence for virion-associated lipid rafts. J. Virol. 77, 8237–8248.

Hapala, I., Kavecansky, J., Butko, P., Scallen, T.J., Joiner, C., Schroeder, F., 1994. Regulation of membrane cholesterol domains by sterol carrier protein-2. Biochemistry 33, 7682–7690.

Haughey, N.J., Holden, C.P., Nath, A., Geiger, J.D., 1999. Involvement of inositol 1,4,5-trisphopate-regulated stores of intracellular calcium in calcium dysregulation and neuron cell death caused by HIV-1 protein tat. J. Neurochem. 73, 1363–1374.

Heise, C., Dandekar, S., Pradeep, K., Duplantier, R., Donovan, R.M., Halsted, C.H., 1991. Human immunodeficiency virus infection of enterocytes and mononuclear cells in human jejunal mucosa. Gastroenterology 100, 1521–1527.

Heise, C., Vogel, P., Miller, C.J., Dandekar, S., 1993. Distribution of SIV infection in the gastrointestinal tract of rhesus macaques at early and terminal stages of AIDS. J. Med. Primatol. 22, 187–193.

Huang, H., Ball, J.M., Billheimer, J.T., Schroeder, F., 1999. Interaction of the N-terminus of sterol carrier protein 2 with membranes: role of membrane curvature. Biochem. J. 344, 593–603.

Huang, H., Schroeder, F., Zeng, C.Q.Y., Estes, M.K., Schoer, J., Ball, J.M., 2001. Membrane interactions of a novel viral enterotoxin: rotavirus nonstructural glycoprotein NSP4. Biochemistry 38, 13231–13243.

Hunter, E., Swanstrom, R., 1990. Retrovirus envelope glycoproteins. In: Swanstrom, R., Vogt, P.K. (Eds.), Retroviruses: Strategies of Replication. Springer-Verlag, Berlin, pp. 187–253.

Kaur, A., Grant, R.M., Means, R.E., McClure, H., Feinber, M., Johnson, R.P., 1998. Diverse host responses and outcomes following simian immunodeficiency virus SIVmac239 infection in sooty mangabeys and rhesus macaques. J. Virol. 72, 9597–9611.

Kestler, H.W., Kodama, T., Ringler, D., Marthas, M., Pedersen, N., Lack-

ley, L.S., Regier, D., Sehgal, P.K., Daniel, M.D., King, N.W., 1990. Induction of AIDS in rhesus monkeys by molecularly cloned simian immunodeficiency virus. Science 248, 1109–1112.

Kirchhoff, F., Carl, S., Sopper, S., Sauermann, U., Matz-Rensing, K., Stahl-Hennig, C., 1999. Selection of the R17Y substitution in SIVmac239 nef coincided with a dramatic increase in plasma viremia and rapid progression to death. Virology 254, 61–70.

Kliger, Y., Gallo, S.A., Peisajovich, S.G., Munoz-Barroso, I., Avkin, S., Blumenthal, R., Shai, Y., 2001. Mode of action of an antiviral peptide from HIV-1. J. Biol. Chem. 276, 1391–1397.

Lambl, B.B., Federman, M., Pleskow, D., Wanke, C.A., 1996. Malabsorption and wasting in AIDS patients with microsporidia and pathogen-negative diarrhea. AIDS 10, 739–744.

Lark, L.R., Berzofsky, J.A., Gierasch, L.M., 1989. T-cell antigenic peptides from sperm whale myoglobin fold as amphipathic helices: a possible determinant for immunodominance. Pept. Res. 2, 314–321.

Lewis, M.G., Zack, P.M., Elkins, W.R., Jahrling, P.B., 1992. Infection of rhesus and cynomolgus macaques with a rapidly fatal SIV (SIVsmm/PBj) isolate from sooty mangabeys. AIDS Res. Hum. Retroviruses 8, 1631–1639.

Lipka, G., Schulthess, G., Thurnhofer, H., Wacker, H., Wehrli, E., Zeman, K., Weber, F.E., Hauser, H., 1995. Characterization of lipid exchange proteins isolated from small intestinal brush border membrane. J. Biol. Chem. 270, 5917–5925.

Lou, W., Peterlin, M., 1997. Activation of the T-cell receptor signaling pathway by nef from an aggressive strain of simian immunodeficiency virus. J. Virol. 71, 9531–9537.

Margolit, H., Spouge, J.L., Cornette, J.L., Cease, K.B., Delisi, C., Berzofsky, J.A., 1987. Prediction of immunodominant helper T cell antigenic sites from the primary sequence. J. Immunol. 138, 2213–2229.

Medina, I., Ghose, S., Ben-Ari, Y., 1999. Mobilization of intracellular calcium stores participates in the rise of $[Ca^{2+}]_i$ and the toxic actions of the HIV coat protein gp120. Eur. J. Neurosci. 11, 1167–1178.

Missiaen, L., Van Acker, K., Parys, J.B., De Smedt, H., Van Baleen, K., Weidema, A.F., Vanoevelen, J., Raeymaekrs, L., Callewaert, G., Rizzuto, R., Wuytack, F., 2001. Baseline cytosolic Ca^{2+} oscillations derived from a non-endoplasmic reticulum Ca^{2+} store. J. Biol. Chem. 276, 39161–39170.

Misumi, S., Endo, M., Mukai, R., Tachibana, K., Umeda, M.M., Honda, T., Takamune, N., Shoji, S., 2003. A novel cyclic peptide immunization strategy for preventing HIV-1/AIDS infection and progression. J. Biol. Chem. 278, 32335–32343.

Naidu, Y.M., Kestler III, H.W., Li, Y., Butler, C.V., Silva, D.P., Schmidt, D.K., Troup, C.D., Sehgal, P.K., Sonigo, P., Daniel, M.D., Desrosiers, R.C., 1988. Characterization of infectious molecular clones of simian immunodeficiency virus (SIV_mac) and human immunodeficiency virus type 2: persistent infection of rhesus monkeys with molecularly cloned SIV_mac. J. Virol. 62, 4691–4696.

Nehete, P.N., Vela, E.M., Hessian, M.M., Sarkar, A.K., Ahi, N., Santini, J., Sastry, K.J., 2002. A post-CD4-binding step involving interaction of the V3 region of viral gp120 with host cell surface glycosphingolipids is common to entry and infection by diverse HIV-1 strains. Antiviral Res. 56, 233–251.

Nelson, J.A.E., Baribaud, F., Edwards, T., Swanstrom, R., 2000. Patterns of changes in human immunodeficiency virus type 1 V3 sequence populations late in infection. J. Virol. 74, 8494–8501.

Parker, J.M.R., Guo, D., Hodges, R.S., 1986. New hydrophilicity scale derived from high-performance liquid chromatography peptide retention data: correlation of predicted surface residues with antigenicity and X-ray derived accessible sites. Biochemistry 25, 5425–5432.

Prochiantz, A., 2000. Messenger proteins: homeoproteins, tat and others. Curr. Opin. Cell Biol. 12, 400–406.

Reed, L.J., Muench, H., 1938. A simple method of estimating fifty per cent endpoints. Am. J. Hyg. 27, 493–497.

Rooney, T.A., Thomas, A.P., 1993. Intracellular calcium waves generated by Ins(1,4,5)P3-dependent mechanisms. Cell Calcium 14, 674–690.

Sakaida, H., Hori, T., Yonezawa, A., Sato, A., Isaka, Y., Yoshie, O., Hattori, T., Uchiyama, T., 1998. T-tropic human immunodeficiency virus type 1 (HIV-1)-derived V3 loop peptides directly bind to CXCR-4 and inhibit T-tropic HIV-1 infection. J. Virol. 72, 9763–9770.

Sanderson, M.J., Charles, A.C., Dirksen, E.R., 1990. Mechanical stimulation and intercellular communication increases intracellular Ca2+ in epithelial cells. Cell Regul. 1, 585–596.

Sanderson, M.J., Charles, A.C., Boitano, S., Dirksen, E.R., 1994. Mechanisms and function of intracellular calcium signaling. Mol. Cell. Endocrinol. 98, 173–187.

Sawai, E.T., Khan, I.H., Montbriand, P.M., Peterlin, B.M., Cheng-Mayer, C., Luciw, P.A., 1996. Activation of PAK by HIV and SIV Nef: importance for AIDS in rhesus macaques. Curr. Biol. 6, 1519–1527.

Schroeder, F., Barenholz, Y., Gratton, E., Thompon, T.E., 1987. A fluorescence study of dehydroergosterol in phosphatidylcholine bilayer vesicles. Biochemistry 26, 2441–2448.

Sharon, M., Gorlach, M., Levy, R., Hayek, Y., Anglister, J., 2002. Expression, purification, and isotope labeling of a gp120 V3 peptide and production of a Fab from a HIV-1 neutralizing antibody for NMR studies. Protein Expression and Purification 24, 374–383.

Shoemaker, K.R., Kim, P.S., Brems, D.N., Marqusee, S., York, E.J., Chaiken, I.M., Stewart, J.M., Baldwin, R.L., 1985. Nature of the charged-group effect on the stability of the C-peptide helix. Proc. Natl. Acad. Sci. U.S.A. 82, 2349–2353.

Shorte, S.L., Faught, W.J., Frawley, L.S., 2000. Spontaneous calcium oscillatory patterns in mammotropes display non-random dynamics. Cell Calcium 28, 171–179.

Steinberg, T.H., Newman, A.S., Swanson, J.A., Silverstein, S.C., 1987. Macrophages possess probenecid-inhibitable organic anion transporters that remove fluorescent dyes from the cytoplasmic matrix. J. Cell Biol. 105, 2685–2702.

Stolowich, N.J., Frolov, A., Atshaves, B.P., Murphy, E.J., Jolly, C.A., Billheimer, J.T., Scott, A.I., Schroeder, F., 1997. The SCP-2 fatty acid binding site: an NMR, circular dichroic, and fluorescent spectroscopic determination. Biochemistry 36, 1719–1729.

Swaggerty, C.L., Frolov, A., McArthur, M.J., Cox, V., Tong, S., Compans, R.W., Ball, J.M., 2000. The envelope glycoprotein of simian immunodeficiency virus contains an enterotoxin domain. Virology 277, 250–261.

Swanstrom, R., Wills, J.W., 1997. Synthesis, assembly, and processing of viral proteins. In: Coffin, J.M., Hughes, S.H., Varmus, H.E. (Eds.), Retroviruses. Cold Spring Harbor Laboratory Press, NY, pp. 263–334.

Ullrich, R., Zeitz, M., Heise, W., L'age, M., Hoffken, G., Riecken, E.O., 1989. Small intestinal structure and function in patients infected with human immunodeficiency virus (HIV): evidence for HIV-induced enteropathy. Ann. Intern. Med. 111, 15–21.

Villalobos, C., Faught, W.J., Frawley, L.S., 1998. Dynamic changes in spontaneous intracellular free calcium oscillations and their relationship to prolactin gene expression in single, primary mammotropes. Mol. Endocrinol. 12, 87–95.